Chemical Engineering Science 188 (2018) 97–111

Contents lists available at ScienceDirect

Chemical Engineering Science

journal homepage: www.elsevier.com/locate/ces

Heat transfer in packed-beds of agricultural waste with low rates of air flow applicable to solid-state fermentation

Fernanda Perpétua Casciatori [a,*], João Cláudio Thoméo [b]

[a] Chemical Engineering Department, Federal University of São Carlos (UFSCar), Rod. Washington Luiz km 235 SP 310, Bairro Monjolinho, 13565-905 São Carlos, SP, Brazil
[b] Food Engineering and Technology Department, Institute of Biosciences, Letters and Exact Sciences, São Paulo State University (UNESP), Cristóvão Colombo 2265, Jardim Nazareth, 15054-000 São José do Rio Preto, SP, Brazil

HIGHLIGHTS

- Paper addressed heat transfer in beds packed with agricultural waste.
- Air flow rate and bed height markedly affected radial temperature profiles.
- Beds of sugarcane bagasse are non-favorable for heat transfer.
- Mixture of particles of different shapes and sizes improves heat transfer.
- Thermal parameters are useful for reliable simulation of bioreactors.

GRAPHICAL ABSTRACT

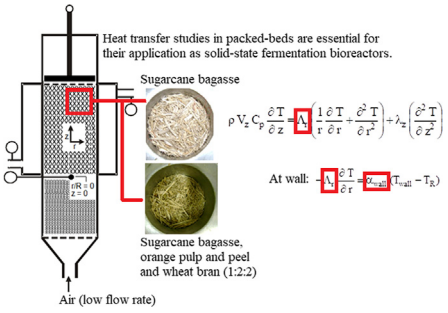

ARTICLE INFO

Article history:
Received 6 March 2018
Received in revised form 19 April 2018
Accepted 15 May 2018
Available online 17 May 2018

Keywords:
Heat transfer
Packed-beds
Bioreactors
Solid-state fermentation
Solid waste

ABSTRACT

Heat transfer studies were carried out in packed-beds (PBs) heated by the wall and percolated by low air flow rates. Porous media were composed by particles of sugarcane bagasse (SCB) and by a mixture of particles of SCB, orange pulp and peel (OPP) and wheat bran (WB) at proportion SCB:OPP:WB 1:2:2 w/w (composed medium), agricultural waste used as substrates in bioreactors of solid-state fermentation (SSF), an interesting biotechnological application of PBs. Once metabolic heat generated has to be dissipated, heat transfer studies and thermal parameters are required. Tube-to-particle diameter ratio was $D/d_p = 260$, bed height ranged from L = 60 to 180 mm, while air flow rate ranged from 400 to 1200 L/h. Air temperature was 40 °C and wall temperature 65 °C. The outlet bed temperatures (T_L) were measured by ring-shaped sensors and by aligned thermocouples. Average temperatures (T_{avg}) and global heat transfer coefficients (U) were calculated separately for central region of the beds and for wall-vicinity. Radial effective thermal conductivity (Λ_r) and wall-to-fluid convective heat transfer coefficient (α_{wall}) have been estimated by means of the traditional two-parameters model. Radial temperature profiles at bed outlet were flattened in the central region and convergent at the edge of the packs. The two-regions approximation for U calculations showed to be appropriate for both packs. Global coefficient U, thermal conductivity Λ_r and convective coefficient α_{wall} increased with increasing air flow rate and decreased with bed height. Λ_r tended to the stagnant value of the thermal conductivity and α_{wall} were lower than 50 $W/m^2/°C$, addressing the difficulty on removing metabolic heat from PBs of SSF.

1. Introduction

The study of heat transfer in fixed beds packed with a porous solid matrix percolated by a fluid is basic for comprehension of

* Corresponding author.
E-mail address: fernanda.casciatori@ufscar.br (F.P. Casciatori).

https://doi.org/10.1016/j.ces.2018.05.024
0009-2509/

thermal phenomena in particulate systems, which are widely used in important unit operations in chemical and food industries. Applications examples include the use of packed-beds (PBs) as separators, absorbers, dryers, filters and heat exchangers (Thoméo and Freire, 2012; Wen and Ding, 2006), besides to be very frequently used as chemical and biochemical reactors, where strongly exothermic irreversible reactions take place. For reactors, the study of heat transfer become even more relevant, once the knowledge of temperature profiles is necessary for a better understanding of chemical and biochemical reactions rates and yields (Thoméo et al., 2004).

A specific application of this kind of fixed beds is their use as packed-bed bioreactors (PBBs) for solid-state fermentation (SSF), a biotechnological process in which agro-industrial by-products are applied as substrates to produce high-added value products, such as several types of enzymes. In other words, by means of SSF, primary or secondary biotechnologically interesting metabolites are released as consequence of the metabolic activities of microorganisms cultivated on a moist solid porous matrix. The water content does not exceed the water retention capacity of the porous media, hence there is no dripping water filling the inter-particle spaces, which in turn are filled with a continuous gas-phase (Durand et al., 1998; Pandey, 1992).

In PBB for SSF, heat transfer studies are also essential, once it is necessary to dissipate the metabolic heat generated by the respiration of the microorganism along the cultivation, in order to maintain the ideal operational conditions for microbial growth and consequent release and preservation of the interesting metabolites (Mitchell et al., 2000). Concerning the airflow rates in SSF systems, although higher airflow rates could be expected to improve metabolically generated heat removal from inside the PBB during the cultivations (Ghildyal et al., 1994), low airflow rates are usually applied due to avoiding the drying of the porous media because of air percolation, which might harm the microbial growth (Casciatori et al., 2016).

The mathematical modeling of heat transfer mechanisms in beds packed with particles from agricultural waste commonly used as substrates in SSF and the simulation of such fermentative systems by solving the models are shown as useful tools for designing and controlling SSF bioreactors. By means of modeling and simulation, it is possible to predict thermal profiles and probable hot spots along the cultivations, as well as to propose operational alternatives on how to avoid overheating within the PBBs (Casciatori et al., 2016; Fanaei and Vaziri, 2009; Mitchell et al., 1999; Sangsurasak and Mitchell, 1995a; 1995b; 1998; Saucedo-Castañeda et al., 1990; Von Meien and Mitchell, 2002).

Such models depend fundamentally on the knowledge of the thermal properties of the porous matrices used as substrates and percolated by air. However, experimental information required by the models are still scarce in literature (Ashley et al., 1999), leading to the use of very hard considerations that consequently give simulated results far from the experimental ones. In this context, the current paper addresses the determination of the radial effective thermal conductivity (Λ_r) and of the convective heat transfer coefficient wall-to-fluid (α_{wall}) in fixed beds percolated by low airflow rates and packed with porous matrices interesting to SSF, aiming to provide thermal parameters values close to the experimental reality for the heat transfer models in SSF systems, aiming to increase the accuracy of simulation of such processes.

Two porous matrices have been studied in the current paper: the first one composed by sugarcane bagasse (SCB) and the second one composed by a mixture of sugarcane bagasse (SCB), orange pulp and peel (OPP) and wheat bran (WB) at proportion SCB:OPP:WB 1:2:2 w/w. The use of SCB in SSF is common and feasible mainly in Brazil, where this by-product of sugar and alcohol industry is abundant, and it has low commercial value (Soccol, 1995). Besides the economic advantages, SCB is a good source of cellulosic carbon, inducing the production of cellulolytic enzymes by the microorganism cultivated, as well as it has a fibrous structure, resulting in porous matrices with high porosity, which is desirable in PBs applied to SSF because of allow appropriate supply of oxygen to the microorganism within the bed.

The composed media SCB:OPP:WB 1:2:2 w/w here studied was employed by several authors to produce by SSF pectinolytic enzymes, largely used in food industry, mainly citric juices industries (Martin et al., 2004, 2010; Umsza-Guez, 2009). Once there is a great interest in the scale-up of this production, engineering studies giving support to the development of pilot and industrial bioreactors are required, justifying the determination of thermal parameters of beds packed with the agricultural waste chosen in the current paper.

1.1. Effective thermal properties of porous media percolated by air

The effective thermal properties of a porous medium percolated by air, such as Λ_r and α_{wall} studied in this paper, comprise several heat transport mechanisms: heat conduction trough the solid particles, heat conduction trough the liquid stagnated in contact with the particles, convection particle-fluid, thermal dispersion in fluid phase, heat conduction between wall and particles and convection wall-to-fluid (Laurentino, 2007; Thoméo, 1990). In general, such effective thermal parameters are obtained by means of experimental spatial profiles of temperatures followed by non-linear parameters fitting.

There are two ways of modeling thermal phenomena in PBB: the two-phase or heterogeneous or the single-phase or pseudo-homogeneous approaches. The two-phase model comprises a specific equation for each phase, by considering either solid and gas phases have specific dynamics of heat transfer. However, this model is difficult to be applied, due to the problems on the experimental measurement of the temperature in each phase (Kunii and Suzuki, 1967). With computational advances, many papers have been published by applying CFD (Computational Fluid Dynamics) tools, which enables to estimate heat transfer coefficients by simulation employing the two-phase model, although it is not possible to make experimental validation (Augier et al., 2010; Guardo et al., 2005).

The one-phase model considers that, for a representative volume element of the pseudo-homogeneous medium, the temperatures of both phases are the same, which simplifies the experimental measurements, once it is enough to be measured the fluid temperature for the thermal parameters of this model can be determined. Controversial issues of this approach are the level of details of the model (Coberly and Marshall, 1951; De Wash and Froment, 1972; Dixon, 1985), the boundary conditions of the energy balance (Dixon, 1985), the way of thermal coefficients estimative and the techniques of temperatures measurements (Thoméo et al., 2004).

Among the first studies of heat transfer in cylindrical packed-beds with monophasic flow, we find the one carried out by Colburn (1931), who measured only average radial temperatures at fluid inlet and outlet. With this, the author determined the global coefficient of heat transfer (U), defined in Eq. (1):

$$\frac{R}{2} G C_p \frac{dTavg}{dz} = U(Tavg - T_{wall}) \quad (1)$$

where R is the total radius of the bed; G is the surface mass flux of the percolating fluid and C_p its specific heat capacity; T_{avg} is the dependent variable average radial temperature; z is the independent variable axial position and T_{wall} is the tube-wall temperature, established by the cooling or heating jacket.

The boundary condition usually employed to solve Eq. (1) is:

$$For\ z = 0,\ T = T_0\ (flat) \tag{1a}$$

The analytical solution of Eq. (1) by applying the boundary condition (1a) is given by Eq. (2):

$$\ln\left(\frac{T_{avg} - T_p}{T_0 - T_p}\right) = \frac{2U}{RGC_p}z \tag{2}$$

This formulation is one-dimensional, once it contemplates only axial temperature profiles along the bed, being particularly useful when radial temperature profiles are almost flat. Eq. (2) has practical application when it is intended to evaluate the total amount of heat added to or removed from the bed, that it is possible by using the global coefficient U.

However, for short beds, it has been observed that the average temperatures calculated from this formulation were markedly different of the measured temperatures, once temperature radial profiles were non-flat (Coberly and Marshall, 1951). For such cases, it has been proposed the two-dimensional formulation of the energy balance or total energy equation, that provides a more detailed thermal profile. For cylindrical beds, this formulation is given by Eq. (3):

$$\rho V_z C_p \frac{\partial T}{\partial z} = \Lambda_r\left(\frac{1}{r}\frac{\partial T}{\partial r} + \frac{\partial^2 T}{\partial r^2}\right) + \lambda_z\left(\frac{\partial^2 T}{\partial z^2}\right) \tag{3}$$

where ρ is the density of the flowing fluid, V_z its axial surface velocity and C_p its specific heat capacity; r and z are variables positions radial and axial, respectively; T is the variable temperature; and Λ_r and λ_z are the effective thermal conductivities in radial and axial directions, respectively.

Into Eq. (3), some assumptions are implicit: steady-state heat transfer and cylindric symmetry of the thermal radial profile. Although this equation is the most complete way of representing the problem, the second derivative of T as a function of z decreases very quickly with the increase of bed height, in a way that the axial dispersion term as a whole (second term at right hand side of Eq. (3)) becomes negligible in comparison to the radial dispersion term (first term at right hand side of Eq. (3)). On this, usually the axial dispersion of heat is neglected. Hence, it is eliminated the parameter λ_z, which is difficult to estimate due to this difference of magnitude order of axial and radial thermal dispersions.

Therefore, the simplified energy equation is obtained, for which the following boundary conditions are applied:

$$For\ z = 0,\ T = T_0 \tag{3a}$$

$$For\ r = 0,\ \frac{\partial T}{\partial r} = 0 \tag{3b}$$

$$For\ r = R,\ -\Lambda_r\frac{\partial T}{\partial r} = \alpha_{wall}(T_{wall} - T_R) \tag{3c}$$

where α_{wall} is the convective wall-to-fluid heat transfer coefficient; T_R is the temperature at r = R (interface porous matrix and tube-wall); R is the total radius of the bed; T_{wall} is the tube-wall temperature, established by the cooling or heating jacket; and T_0 is the temperature of the air at z = 0 (bed-inlet).

The integration of the simplified energy equation with boundary conditions (3a) to (3c) gives the traditional two-parameters (Λ_r and α_{wall}) model (Coberly and Marshall, 1951), whose analytical solution is given in Eq. (4):

$$\frac{T_{wall} - T}{T_{wall} - T_0} = \sum_{n=1}^{\infty}\frac{2NiJ_0(\gamma_n r/R)}{[Ni^2 + \lambda_n^2]J_0(\gamma_n)}\exp\left[-\frac{\Lambda_r\gamma_n^2}{\rho V_z C_p R^2}z\right] \tag{4}$$

where $Ni = (\alpha_{wall}\ R/\Lambda_r)$ is the modified Biot number; J_0 is the 1st specie and zero order Bessel function; and γn are the characteristic eigen-values which satisfy the following transcendental equation, where J_1 is the 1st specie and 1st order Bessel function:

$$NiJ_0(\gamma_n) - \gamma_n J_1(\gamma_n) = 0 \tag{4a}$$

Several authors (De Wash and Froment, 1972; Dixon, 1985; Smirnov et al., 2003; Thoméo, 1995) used Eq. (4) to determine values of Λ_r and α_{wall} by applying the non-linear minimum square method. The same procedure will be followed in the current paper. Those authors observed Λ_r depended on bed height, presenting high values near the bed inlet and decaying asymptotically to a constant value with the increase of bed height. For α_{wall}, the dependence on bed height is not defined, once it presents high values near bed inlet, but the decay is non-regular with bed height increase. Generally, literature reports a linear dependence of both parameters on the flowrate of the fluid (Tsotsas, 2010).

2. Material and methods

2.1. Particles

Sugar cane bagasse (SCB) and a mixture of SCB, orange pulp and peel (OPP) and wheat bran (WB) at proportion SCB:OPP:WB 1:2:2 w/w (composed medium) were the particles used in the compositions of the porous matrices here studied.

The raw materials were abundantly washed with tap water to remove filth and oven dried at 65 °C until constant weight. SCB was kindly provided by Usina Vale (Onda Verde-SP, Brazil), an industrial ethanol and sugar producer. Only fibers restrained between 3 and 1.44 mm opening sieves were used. OPP was kindly provided by Citrovita (Catanduva-SP, Brazil), an industrial orange juice producer. This material was ground in knife mill and only the particles restrained between 2 and 1.44 mm opening sieves were used. WB was bought in a local retailer (Cerealista Alvorada, São José do Rio Preto-SP, Brazil) and it was not sieved.

Randomly, 50 fibers of SCB were chosen for measurement with a caliper. The mean value of the measurements of thickness of the fibers resulted at the mean particle diameter d_p = 0.177 mm (±0.153 mm), used as characteristic dimension for the thermal parameters calculations. This same value has been used for the composed medium, once the volumetric fraction of the SCB fibers is much higher than the one of OPP and WB.

2.2. Experimental set-up

The equipment constructed for this work is illustrated in Fig. 1a and it is similar to experimental set-ups formerly used for heat transfer studies in non-reactional PBs (Thoméo et al., 2004; Thoméo and Freire, 2000; Thoméo and Grace, 2004). Air supplied by a compressor percolated through the beds. The pressure in the line was regulated by a pressure regulator equipped with a filter, which intercepted oil and dirt. The air flow rate was stablished by a needle valve and monitored by a rotameter. Before entering in the bed, the air temperature was adjusted by passing through a column filled with glass beads placed within a thermostatic bath at 40 °C. After percolating through the bed, the air was vented to the atmosphere.

Fig. 1b shows the thermal measuring cell. The entrance section was made of stainless-steel of 46.7 mm diameter and 90 mm length. The heating section was composed of two concentric stainless-steel tubes of 46.7 mm internal diameter (D) and 70 mm external diameter, both 210 mm in length. The annular space between them was used as a jacket, through which water, kept at a constant temperature of 65 °C by a thermostatic bath, was circulated. Wall-temperature (T_{wall}) was assumed constant and equal to 65 °C, assured by metallic material of the thin internal wall of

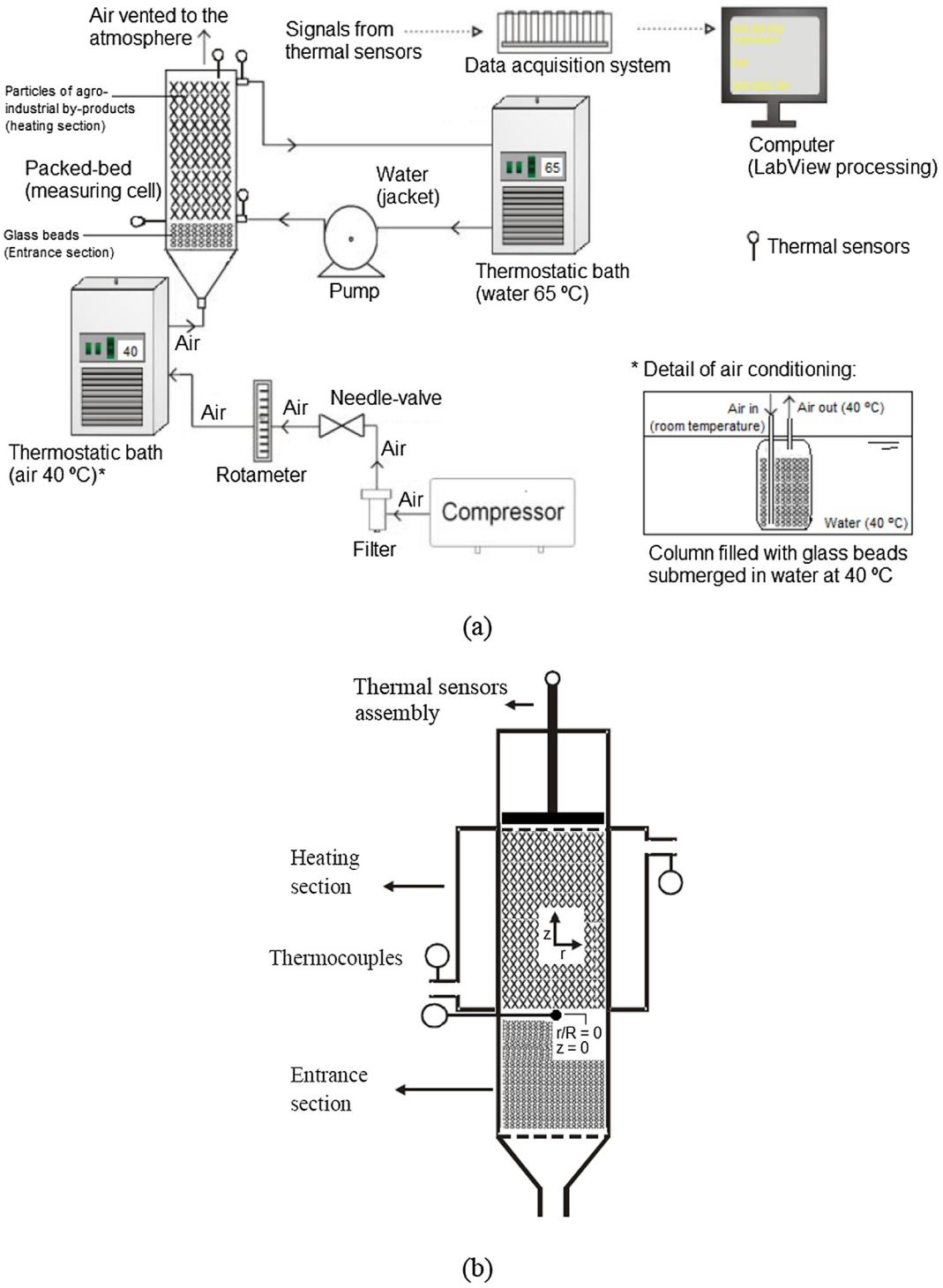

Fig. 1. Experimental set-up: (a) Full-system for heat transfer analysis; (b) Measuring cell.

the heating section, as well by high water flow rate through the jacket.

2.3. Packing of the measuring cell

The entrance section was packed with glass beads of diameter 3 mm and it has been used to develop the air velocity profile. A stainless-steel screen was fixed at the bottom of the entrance section to support the pack. A grid with a mesh opening slightly smaller than the glass beads diameter was employed.

The loose packing method described by Casciatori et al. (2014) was used to densely pack the heating section, within which portions of the particles of agro-industrial by-products (SCB and SCB:OPP:WB 1:2:2 w/w) were added and gently distributed uniformly across the bed surface area after each new addition until a specified bed height has been reached (L = 60, 120 and 180 mm).

SCB, OPP and WB particles were moisturized (up to initial moisture content of 70% w/w, wet basis) and mixed previously to the packing of the composed medium SCB:OPP:WB 1:2:2 w/w within the measuring cell. After packing, the bed was avoided to shake,

preventing local heterogeneities that could appear in case smaller and denser particles of OPP and WB segregate to the bottom of the measuring cell. Preliminary tests of packing within a glass column showed that OPP and WB particles did not sediment even after 5 days of air percolation and consequent drying (up to final moisture content of around 5% w/w, wet basis). Despite the outflow of water from the pack due to drying caused by undersaturated air percolation, OPP and WB particles remained stick in between SCB fibers. Constant bulk densities attested reproducibility of the packing on tests and replicates (Casciatori et al., 2014).

2.4. Temperature measurement technique

Measurements of temperatures were made following the widely used technique of thermocouples above the bed of particles. A set of thermocouples was placed above the top layer of particles, with the sensors located at different radial and angular positions. Measuring the axial temperature profile via this technique required different bed heights.

A device composed of a wood shaft (15 mm in diameter and 200 mm in length), coupled to a sheathed thermocouple, carried the temperature-measuring assemblies (see Fig. 2a). The first temperature-measuring assembly was formed by five sheathed copper-constantan thermocouples (T-type), each stainless-steel sheath being 1.5 mm in outer diameter and 44.55 mm in length (Fig. 2b). These thermocouples, located in five radial positions (r/R = 0; 0.27; 0.56; 0.79 and 0.92), were held in place by a circular nylon plate with large holes in cross (Fig. 2b). The central thermocouple (r/R = 0) was the one coupled to the wood shaft.

The other assembly was a ring-shaped sensor containing four copper rings (Fig. 2c), with a copper-constantan thermocouple soldered onto each ring (Fig. 2c). Each ring had a circular cross section of 1.5 mm diameter. The concentric rings were kept in place by a nylon frame in "Y-shape" (Fig. 2c). Their radial positions were the same as those of the aligned thermocouples, except for the extra central thermocouple (r/R = 0), that was again the one coupled to the wood shaft. The wood shaft helped keeping both set of sensors, aligned or ring-shaped, at the desired heights above the beds.

Because Freiwald and Paterson (1992) reported problems of heat conduction along the thermocouple assembly when it is inside the bed for long periods, the assemblies in this work were placed over the bed only 5 min before the definitive measurements were taken. The distance of the sensor above the bed was kept at 5 mm, as recommended by Thoméo et al. (2004), although the authors also reported that the clearance between the bed surface and temperature sensor did not influence temperature profiles for high D/d_p. In this work, $D/d_p \gg 50$. When the aligned thermocouples were used, they were rotated 360° at intervals of 45°.

Keeping empty the measuring cell (i.e., with no pack within the heating section), measurements of T_0 for each air flow rate were made by a radially inserted sheathed thermocouple at z = 0 and r/R = 0 (Fig. 2b). Signals from all thermal sensors were collected by a data acquisition system (Compaq DAQ, National Instruments, Austin, USA) and sent for a computer to be processed by Lab View 8.5 software (National Instruments, Austin, USA).

2.5. Thermal experiments

Thermal experiments were carried out in duplicate, with definitive measurements of temperatures being taken after steady-state of heat transfer have been achieved. Steady-state was assumed when equal temperatures at all radial and angular positions have been registered after 1 h. In the case of the composed media SCB: OPP:WB 1:2:2 w/w, that had to be packed with high moisture content to avoid particles segregation (as mentioned in item 2.3), steady-state thermal regimes have been achieved only some hours after drying stopped.

Bed heights were L = 60, 120 and 180 mm and air flow rates ranged from 400 to 1200 L/h, comprising air flow rates equivalent to superficial velocities typically used in solid-state fermentation bioreactors (Ghildyal et al., 1994).

2.6. Calculations of average temperatures and thermal parameters

The response variables were the radial temperatures at bed outlet, $T_L = f(r)$, and the average radial temperatures (T_{avg}), obtained by numerical integration of the experimental radial temperatures profiles (T_L) by means of the trapeze rule. The integrations have been done by following three different ways: (a) taking points of T_L from r/R = 0 to 0.92 (central region); (b) taking points of T_L from r/R = 0 to 1 (assuming T_L = 65 °C at the wall, r/R = 1) (full cross-section); and (c) taking points from r/R = 0.92 to 1 (wall-vicinity).

The global coefficient of heat transfer (U) was calculated directly from Eq. (2), employing for T_{avg} the values resulting of the three different ways of integration, as described above. The parameters α_{wall} and Λ_r were calculated by employing the traditional two-parameters model, given in Eq. (4). A Fortran language program, already available and previously used by Thoméo and Freire (2000), was used for fitting the model to the experimental

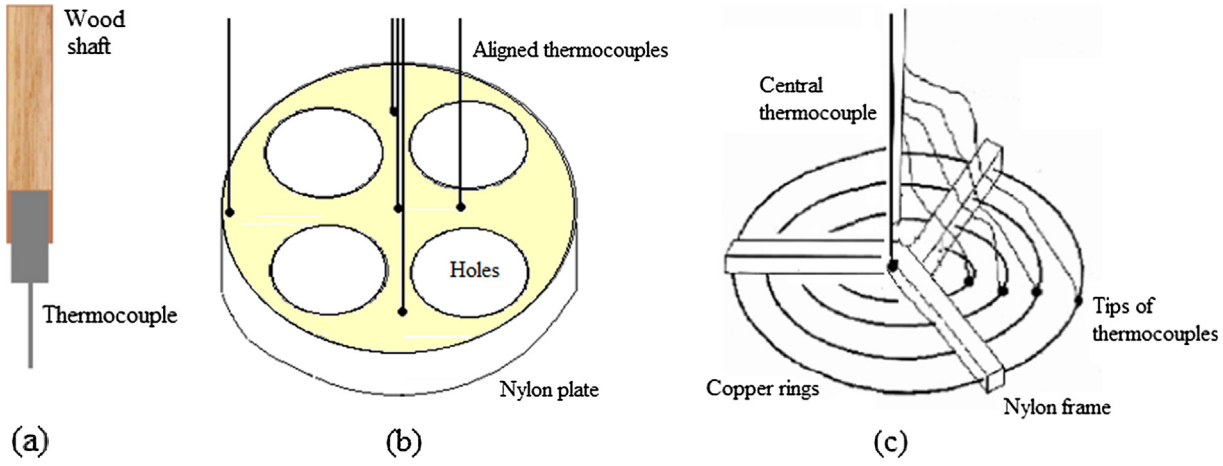

Fig. 2. Thermal sensors assemblies: (a) wood shaft coupled to the central sheathed thermocouple, guide of both thermal sensors assemblies; (b) aligned thermocouples; (c) ring-shaped thermocouples.

data by using the non-linear least square method optimized by Marquardt (1963) algorithm.

3. Results and discussion

3.1. Inlet air temperature, T_0

Although the air passed through a column filled with water and glass beads placed within a thermostatic bath at 40 °C before flowing into the bed, the steady-state temperatures registered by the thermocouple radially inserted at position r/R = 0 and z = 0 (T_0) with the empty cell indicated that T_0 values were always higher than 40 °C, as shown in Table 1. As variation coefficients of five replicates are lower than 1%, we may consider results reproductible.

The radial insertion of the thermocouple is the reason why $T_0 >$ 40 °C. This is due to the so-called fin effect, already discussed by Thoméo et al. (2004). The heat fin effect for radially inserted thermocouple readings appears because heat is transferred from the wall to the bed by the thermocouple sheath. The higher the air flow rate, the more heat is dissipated by convection along the sheath. Hence, fin effect decreases as air flow rate increase, and T_0 gets closer 40 °C. To consider fin effect in thermal parameters estimation, values from Table 1 were used for T_0 in boundary conditions (1a) and (3a) (z = 0) and in Eqs. (2) and (4).

A relation between T_0 and air flow rate (AFR) have been established by fitting of Eq. (5), with exponential decay of T_0 with the independent variable AFR:

$$T_0 = T_{ref} + 6.3\exp(-AFR/636.3) \quad (5)$$

where T_{ref} is the reference temperature (40 °C, set in thermostatic bath) and AFR is given in em L h^{-1}. Fig. 3 presents the experimental data and the fitted curve. At stagnant condition (AFR tends to zero), T_0 tends to 46.3 °C; at very high air flow rates (AFR tending to infinity), T_0 tends to T_{ref}, which is according to the physical phenomenon of convective cooling above discussed. Eq. (5) may be applied in computational programs that require such relation.

3.2. Radial temperature profiles at bed outlet, $T_L = f(r)$

The influence of air flow rate on the measured radial temperatures at bed outlet, $T_L = f(r)$, was assessed using the aligned thermocouples for PBs of SCB and both the aligned thermocouples and the circular ring-shaped sensors for PBs of SCB:OPP:WB 1:2:2 w/w. Radial temperature profiles at bed outlet are shown in Fig. 4a–c, for SCB, and in Fig. 5a–c, for composed medium, for bed heights L = 60, 120 and 180 mm, respectively.

For PBs of SCB with L = 60 and 120 mm, temperature remains almost constant nearby r/R = 0, with mild variation from the central axis up to r/R = 0.56, especially for low air flow rates. The same

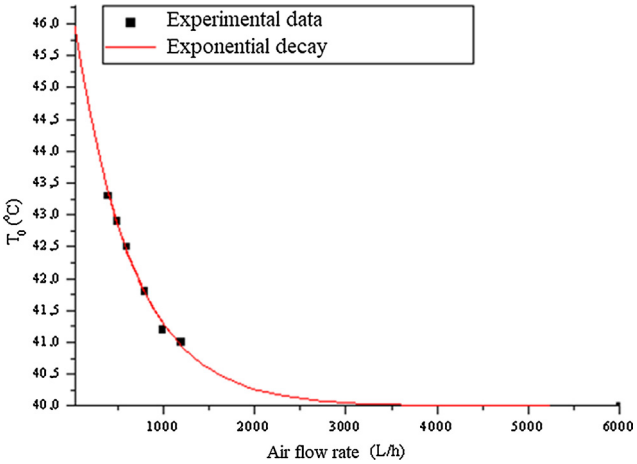

Fig. 3. Relation between air flow rate (AFR) and temperature at z = 0 (T_0).

is true for PBs of SCB:OPP:WB 1:2:2 w/w with L = 60 and 120 mm, although, in a general way, radial temperature profiles were steeper for beds packed with the composed medium in comparison to the ones packed with SCB only. Particularly for the PB of composed medium with L = 180 mm, radial temperature profile was pronounced from r/R = 0 to r/R = 0.92, with gradients superior to 10 °C. For all the cases, the higher the air flow rate, the lower T_L, once the bed was heated by the wall and cooled by the air percolating.

In some cases, even with a new packing of the measuring cell for the replications, thermocouples placed at r/R = 0.27 and 0.56 registered temperatures inferior to the one registered by the thermal sensor placed at r/R = 0. These points contradict the expected profile of decreasing temperatures from the wall to the center of the bed, once the bed was heated by the wall. However, as thermal profiles were flattened near central axis of the bed, temperature differences at r/R = 0; 0.27 and 0.56 were lower than precision of the sensors (±0.5 °C).

In the case of PBs of SCB, once thermal profiles of T_L were assessed using the aligned thermocouples, one might suspect that fin effect could arise due to temperature gradient along the sheath. As already mentioned, fin effect occurs when the sheath base and the junction of a thermocouple are subjected to different temperatures, leading to heat conduction along the sheath and masking the real value of the temperature (Bird et al., 2002). In the current experiments, if fin effect had to be considered, we may concern that it would be more significant for L = 180 mm, when the end of the sheath containing the junction of the thermocouple stays within the measuring cell, under jacket influence, and the other end is exposed to room temperature. In order to check if the exposure of the sheath to room temperature lead to non-negligible fin effect in T_L measurements, we performed some measurements in

Table 1
Steady-state temperatures at z = 0 (T_0) for airflow rates from 400 to 1200 L/h.

		Airflow rate (L/h)					
		400	500	600	800	1000	1200
T_0 (°C)	Test 1	43.0	42.6	42.3	41.6	41.4	41.3
	Test 2	43.0	42.8	42.5	41.6	41.3	41.2
	Test 3	43.2	42.7	42.4	41.9	41.2	41.0
	Test 4	43.6	43.3	42.6	41.9	41.1	40.9
	Test 5	43.8	43.2	42.7	41.9	41.0	40.8
	Average T_0 (°C)	43.3	42.9	42.5	41.8	41.2	41.0
	CV* (%)	0.8	0.7	0.4	0.4	0.4	0.5

* CV: coefficient of variation.

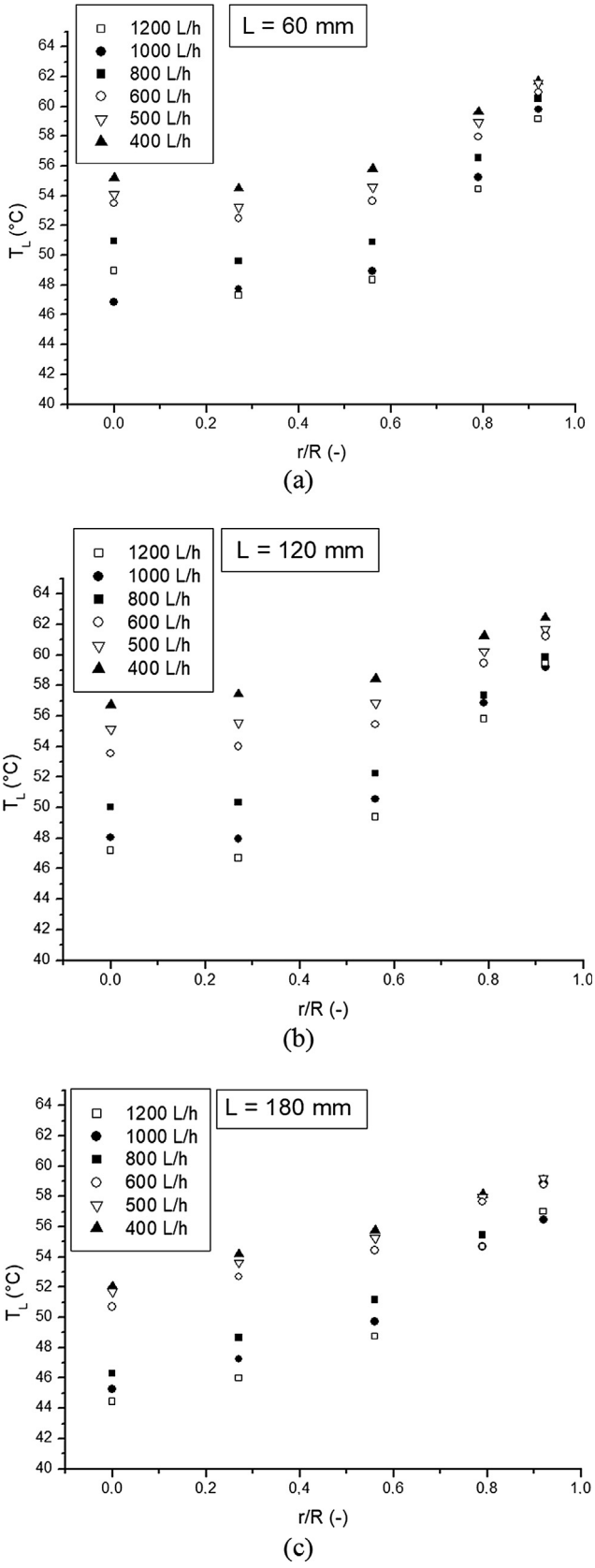

Fig. 4. Effect of air flow rate on measured T_L of packed-beds of sugarcane bagasse: (a) L = 60 mm; (b) L = 120 mm; (c) L = 180 mm.

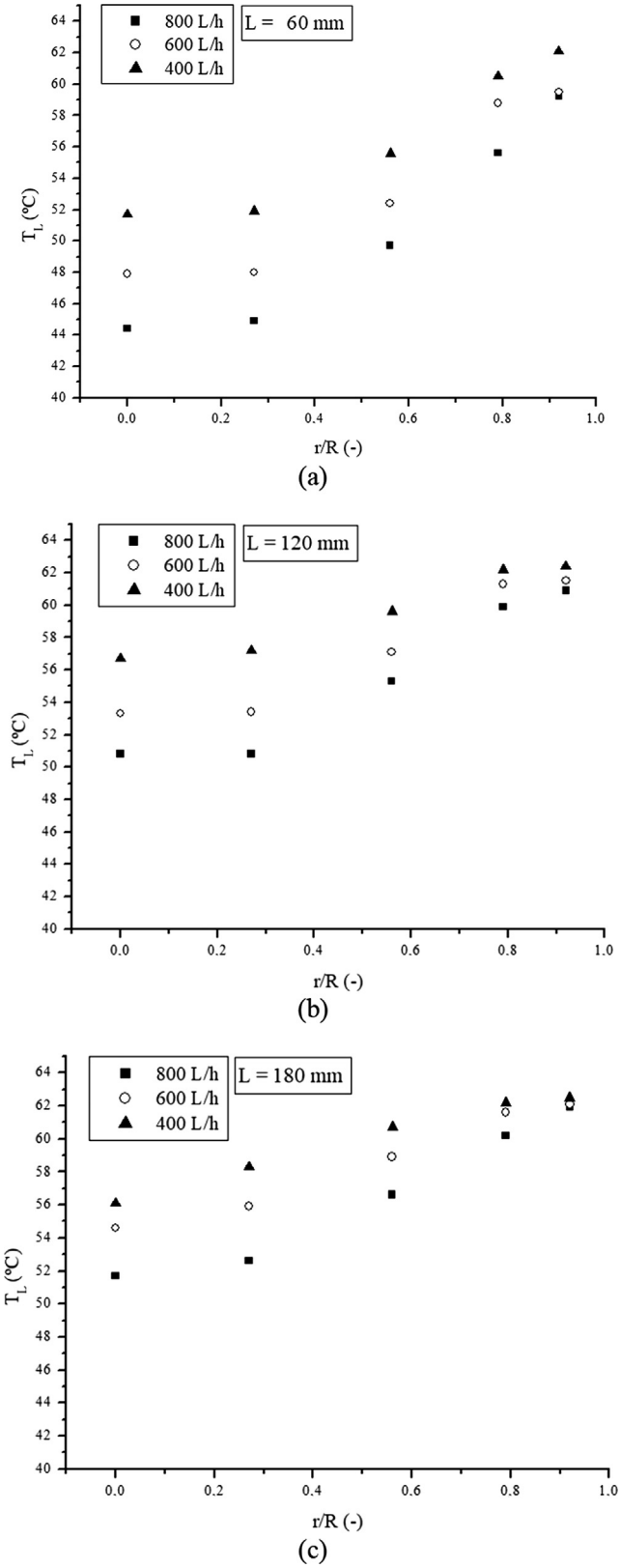

Fig. 5. Effect of air flow rate on measured T_L of packed-beds of composed medium (SCB:OPP:WB 1:2:2 w/w): (a) L = 60 mm; (b) L = 120 mm; (c) L = 180 mm.

two situations for L = 180 mm. In first case, measurements were done with the measuring cell open, with no extension (as usual); in second case, an extension of a plastic tube with 10 cm length was coupled to the top of the measuring cell, avoiding sudden exposure to room temperature. For both the situations, thermal profiles were coincident (data not shown), attesting that fin effect over T_L measurements could be neglected.

For PBs of SCB, a more abrupt temperature variation is observed when air flow rate changes from below 600 to above 800 L/h. This gap in air flow rate has been assumed as the range of transition from a predominant near-stagnant contribution to an equivalence of static and dynamic contributions for heat transfer within the packed-beds.

It is also observed that the nearest-wall measured temperature (T_L at r/R = 0.92) tended, in average, to values near to T_R = 60 °C, for beds of SCB, and to T_R = 61 °C, for beds packed with the composed medium, independent of bed length and air flow rate. Taking into account that the distance from the most external thermal sensor and the bed wall (assumed to be at T_{wall} = 65 °C) was near 1 mm, the temperature gradient in this region was very expressive (up to 5 °C/mm). On this, we may infer that convective boundary condition at r = R is the most appropriate to represent the physical phenomenon near wall and that there is a high thermal resistance between the wall and the edge of the porous matrices here studied.

These high temperature gradients near wall can be attributed to the high porosity clearly observed at the region of contact between the wall and the edge of the porous medium, especially the one composed by SCB dry fibers. This high porosity near wall results from a different level of packing caused by the physical presence of the cell wall, the so-called wall effect (Thoméo et al., 2004; Zotin, 1985). The structure of beds packed with thin wood chips studied by Hamel and Krumm (2008) may be considered similar to the ones of the beds packed with SCB dry fibers. According to those authors, spatial oscillations of porosity of porous media change interstitial air velocities, affecting heat transfer mechanisms and resulting spatial variations of the thermal parameters of PBs. Unlike reported by several authors for PBs of glass beads, the porosity profile of PBs of irregular shaped and deformable particles are not properly oscillatory cushioned (Hamel and Krumm, 2008; Ridgway and Tarbuck, 1968; Zotin, 1985), but there is an accentuated decrease for a constant value at a distance of only 0.5 d_p. In this short gap, porosity is very high, favoring preferential air flow near the wall, the so-called channeling effect, that allows the formation of a boundary layer of heat transfer and justifies the use of the convective boundary condition at r = R, as well as leads to higher temperature gradients. For the PBs of SCB:OPP:WB 1:2:2 w/w, channeling effect was less significant, due to the presence of particles of OPP and WB in between SCB fibers. OPP and WB particles are smaller and more regular than SCB fibers, hence they provide a better contact between the edge of the pack of composed medium and the wall, disturbing the formation of a proper channel near to the wall. Fig. 6a–c presents upper view of PBs of wood chips, of SCB and of SCB:OPP:WB 1:2:2 w/w, respectively, where the above discussed similarities and differences of the channels formed near tube-wall in each case can be clearly seen.

3.3. Average temperatures at bed outlet, T_{avg}

For PBs of SCB, Fig. 7a–c present average temperatures at bed outlet (T_{avg}) as a function of the air flow rate parametrized by bed length and referring, respectively, to integrations over: (a) central region of the bed; (b) full cross-section of the bed; (c) wall-vicinity region of the bed. The same are shown by Fig. 8a–c for PBs of the composed medium SCB:OPP:WB 1:2:2 w/w.

Fig. 7a and b and Fig. 8a and b show T_{avg} increasing with the increase in bed length. Same trend is not indicated by Fig. 7c and Fig. 8c, that instead show that T_{avg} at wall-vicinity does not depend on bed height, for both PBs of SCB and of composed medium. This is due to this region to be almost a gap or a channel, within which temperatures are kept near T_{wall}. In general, T_{avg} is more dependent on air flow rate than on bed length; the higher the air flow rate, the lower T_{avg}, due to convective cooling by air flow.

Comparing the pairs of Fig. 7a and b and Fig. 8a and b, it is seen that the dependence of T_{avg} on air flow rate was similar for integrations over the central region and over the full cross-section of the beds. For integration over the full cross-sections, T_{avg} is around 1 °C higher than for integration up to r/R = 0.92, once the highest temperature of the system (T_{wall}, assumed equal to 65 °C) is inserted for the integration up to r/R = 1 (tube-wall).

On the other hand, Fig. 7c and Fig. 8c reveals that T_{avg} values at wall-vicinity were considerably higher, 5–8 °C above the values observed for central region or full cross-section of the beds. Such result confirms that, near tube-wall, heat transfer mechanism is predominantly convective. As already suggested by Gunn et al. (1987), it may be interesting to determine heat transfer coefficients specifically for wall-vicinity, separately of effective thermal parameters associated with heat transfer across the full cross-section.

Also, T_{avg} values at wall-vicinity are almost the same for PBs of SCB (Fig. 7c) and of composed medium SCB:OPP:WB 1:2:2 w/w (Fig. 8c), what will be reflected in global coefficient (U), despite the channeling effect is less pronounced for the composed medium.

3.4. Global coefficients of heat transfer, U

For PBs of SCB, Fig. 9a–c present global coefficients of heat transfer (U) as a function of the air flow rate parametrized by bed length and referring, respectively, to values obtained by using, in Eq. (2), T_{avg} resulting of integrations over: (a) central region of the bed; (b) full cross-section of the bed; (c) wall-vicinity region of the bed. The same are shown by Fig. 10a–c for PBs of the composed medium SCB:OPP:WB 1:2:2 w/w.

In general, for both porous matrices, the higher bed length, the lower U; this is in accordance with the definition of this parameter, which is based on classical Newton's definition for convective heat

Fig. 6. Upper view of beds packed with different particles: (a) wood chips (extracted from Smirnov et al., 2003); (b) sugarcane bagasse dry fibers; (c) composed medium (SCB:OPP:WB 1:2:2 w/w).

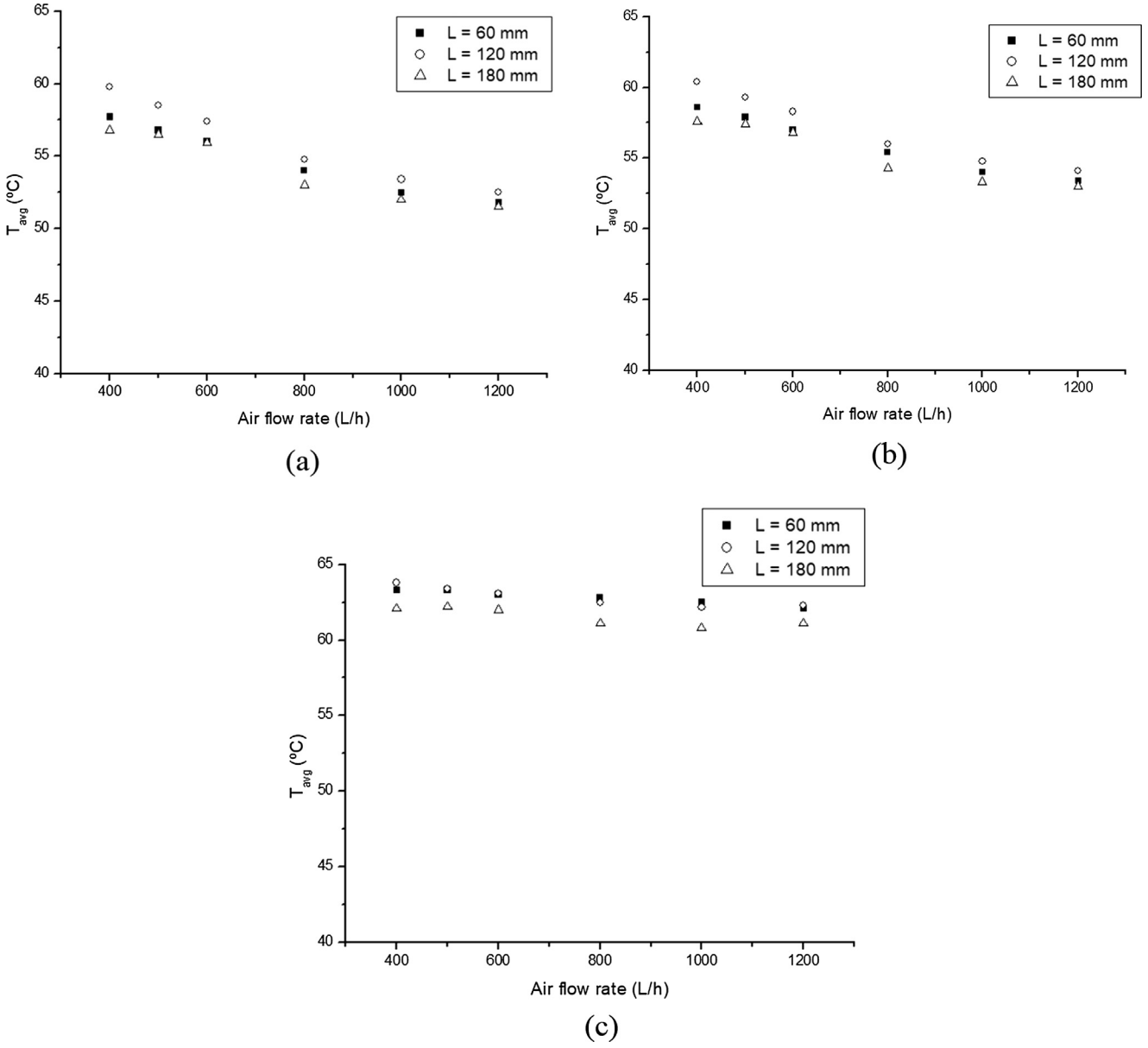

Fig. 7. Average temperatures at outlet of beds of sugarcane bagasse referring to integrations over: (a) central region of the bed; (b) full cross-section of the bed; (c) wall-vicinity region of the bed.

transfer coefficients of fluids flowing inside tubes (Bird et al., 2002). It is also observed that U values were very close for calculations based on T_{avg} calculated from r/R = 0 to 0.92 or to 1 (pairs of Fig. 9a and b for SCB and Fig. 10a and b for composed medium), because the five experimental points integrated over 92% of the full cross-section minimized the influence of the sixth point r/R = 1, T = T_{wall} = 65 °C (assumption).

This global heat transfer coefficient U may be also calculated by correlations similar to the ones employed for convective heat transfer coefficients, as shown in Eq. (6):

$$\frac{U_d}{U_f} = ARe^{b}Pr^{c} \quad (6)$$

where U_f is the global coefficient of heat transfer in the empty tube; U_d is the dynamic global coefficient in the packed-bed; Re is Reynolds number; Pr is Prandtl number of the flowing fluid and A, b and c are fitting constants (Bird et al., 2002). Hence, if U increase when air flow rate increase, it means that dynamic contribution is important. In the current paper, dynamic contribution has been significant only for L = 60 mm, i.e., for short beds.

Concerning U values at wall-vicinity (Fig. 9c and Fig. 10c, respectively, for PBs of SCB and of SCB:OPP:WB 1:2:2 w/w), they clearly increase linearly with air flow rate. Hence, dynamic effects of heat transfer shows to be more expressive near tube-wall, resulting much higher U values (2–3-fold) in comparison to U obtained for the full cross-section, especially for the shorter beds and the higher air flow rates. Therefore, it is convenient to work with separate global coefficients for wall-region and core-region of the beds, or using a model with two regions in order to better represent heat transfer in packed-beds of materials like the agricultural waste here studied.

In Table 2, U calculated for full cross-section and wall-vicinity in PBs of SCB and of composed medium with L = 60 mm are presented and statistically compared. Replications refer to the use of T_{avg} calculated based on radial temperature profiles obtained in duplicate of independent experiments. For U referring to the full cross-

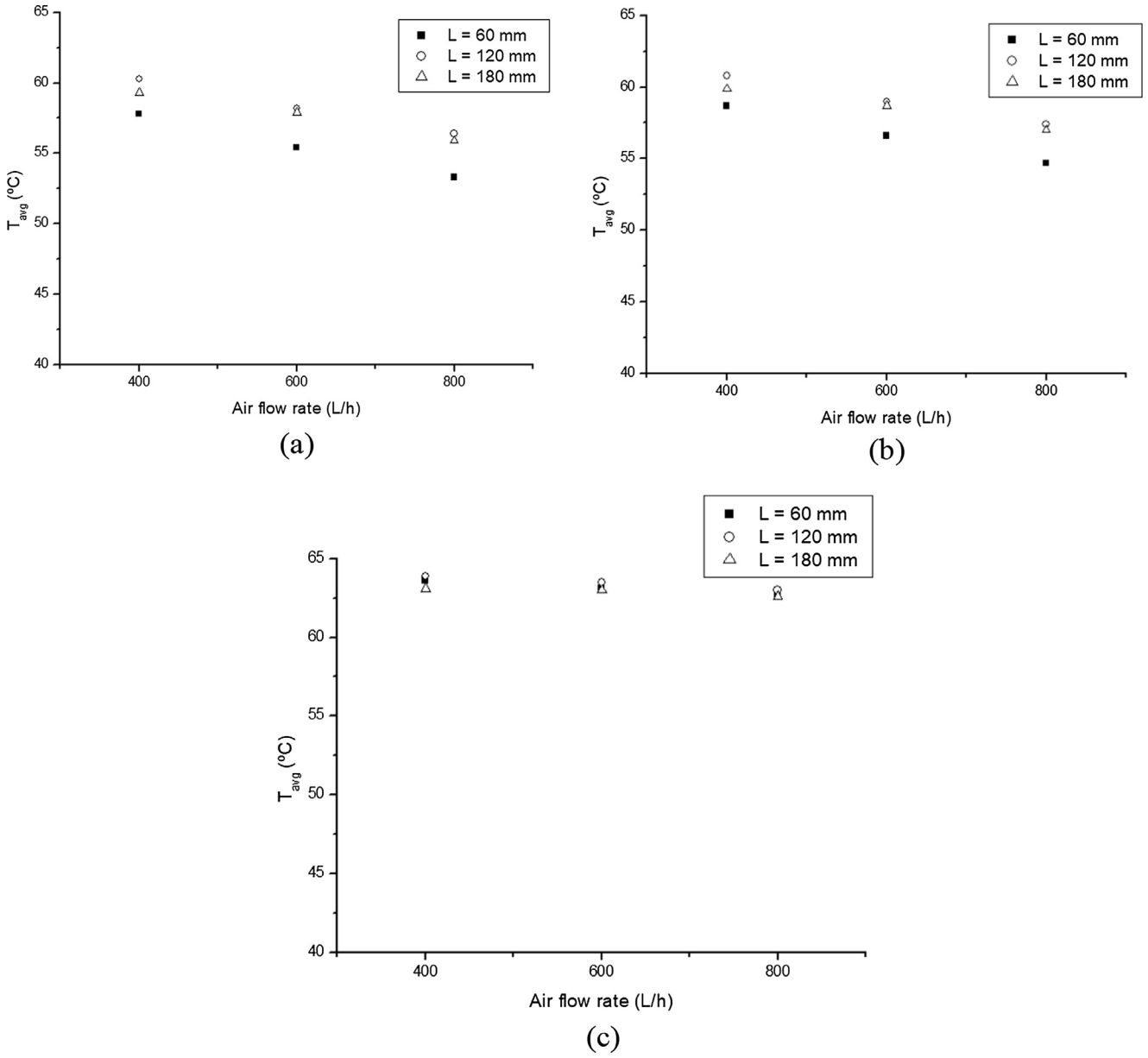

Fig. 8. Average temperatures at outlet of beds of composed medium referring to integrations over: (a) central region of the bed; (b) full cross-section of the bed; (c) wall-vicinity region of the bed.

section, both sources of variations air flow rate and type of porous medium played significant effect on U (significance level $\alpha = 0.05$), with $U_{composed\ medium} < U_{SCB}$. This result is due to thermal gradients to be lower for SCB than for composed medium. In order to represent a more intense heat transfer in PBs of composed medium, their U have to be smaller. On the other hand, variance analysis showed that type of porous medium did not affect significantly U at wall-vicinity, once temperatures at r/R = 0.92 were almost the same for both porous matrices. Also, air flow rate affects more strongly U at wall-vicinity. For bed heights L = 120 and 180 mm, same results for this comparison have been found (data not shown).

Although radial temperature profiles were a bit steeper for PBs of composed medium, the use of U may still be appropriate to predict global quantity of energy to be added to or removed from solid-state fermentation bioreactors. However, for L = 180 mm and air flow rate 800 L/h, temperature difference from r/R = 0 to 0.92 was near 10 °C, making inadequate the use of U, that assumes flat radial temperature profile. Moreover, the one-dimensional model may be not appropriate for simulations of fermentative processes, once there may be a hot spot due to heat generation within a jacketed packed-bed, requiring a two-dimensional model and parameters like Λ_r and α_{wall} for better predictions of heat removal from hot spots.

3.5. Thermal parameters of the two-dimensional model, Λ_r and α_{wall}

Thermal parameters Λ_r and α_{wall} estimated employing the traditional two-parameters model (Eq. (4)) are shown in Tables 3 and 4 for PBs of SCB and of SCB:OPP:WB 1:2:2 w/w, respectively. The calculated relation Λ_r/λ_0 is also presented, where λ_0 is the stagnant effective thermal conductivity, whose values have been taken from Casciatori et al. (2013), that presented stagnant effective thermal conductivities of beds packed with the same porous matrices used in the current work.

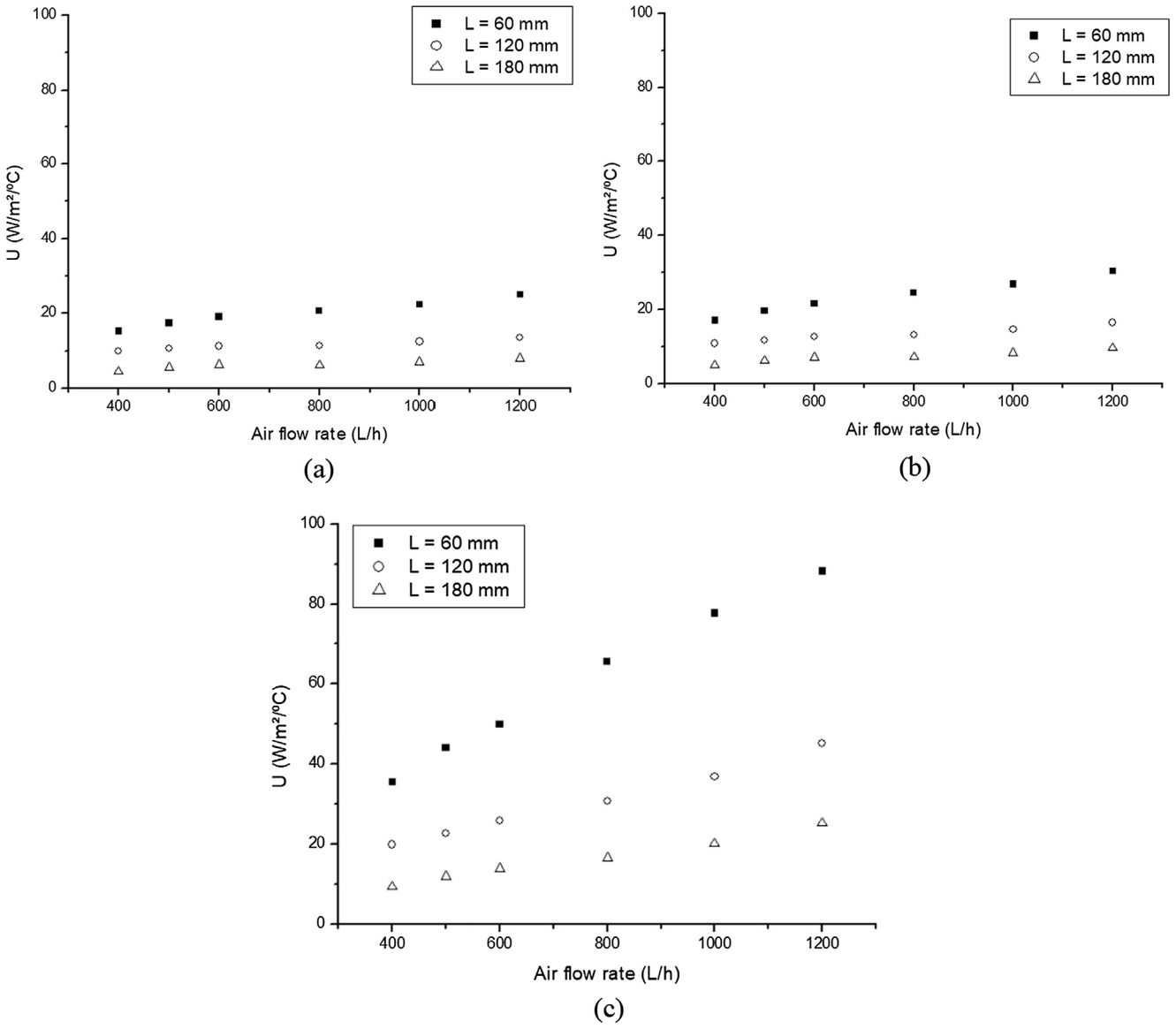

Fig. 9. Global coefficient U at outlet of beds of sugarcane bagasse referring to T_{avg} integrated over: (a) central region of the bed; (b) full cross-section of the bed; (c) wall-vicinity region of the bed.

As it may be seen on Tables 3 and 4, Λ_r presented a trend of increasing with increasing air flow rates and of decreasing with the increase of bed height, as already reported in literature (De Wash and Froment, 1972; Dixon, 1985; Thoméo, 1995), although with inert porous matrices and not with such low air flow rates. At the lower air flow rates here employed, $\Lambda_r/\lambda_0 \rightarrow 1$ for beds with L = 180 mm, for both porous matrices.

Dixon et al. (1978) and Dixon (1997) separated Λ_r into to contributions, one static and one dynamic, as shown in Eq. (7a):

$$\frac{\Lambda r}{\lambda_f} = \frac{\lambda_0}{\lambda_f} + \frac{\lambda_d \mathrm{RePr}}{\mathrm{GC_p d_p}} \tag{7a}$$

where λ_f is the molecular thermal conductivity of the fluid and C_p its specific heat capacity; λ_d is the effective thermal conductivity due to the dynamic contribution; Pr is Prandtl number; G is the air mass flux and Re is Reynolds number, given by Eq. (7b):

$$Re = \frac{V_z\, d_p}{\nu_a} \tag{7b}$$

where d_p is the mean particle diameter; ν_a is the kinematic viscosity of the air and V_z is its axial surface velocity.

It is possible to affirm that, in the case of the PBs studied in the current work under the here chosen operational conditions, static component was predominant over Λ_r on the heat transfer resistance, making $\Lambda_r \rightarrow \lambda_0$. For short beds, this effect is less pronounced, once heat transfer is very intense and the formation of a boundary layer near tube wall disturbs Λ_r values.

The heat transfer model for SSF in PBBs proposed by Sangsurasak and Mitchell (1998) makes the following assumptions for the effective thermal conductivity parameter, Eqs. (8a) and (8b):

$$\Lambda_r = \lambda_z = \lambda_{bed} \tag{8a}$$

$$\lambda_{bed} = (1-\epsilon)\lambda_{particles} + \epsilon\lambda_f \tag{8b}$$

where ε is bed porosity and $\lambda_{particles}$ is the thermal conductivity of the particles of substrate.

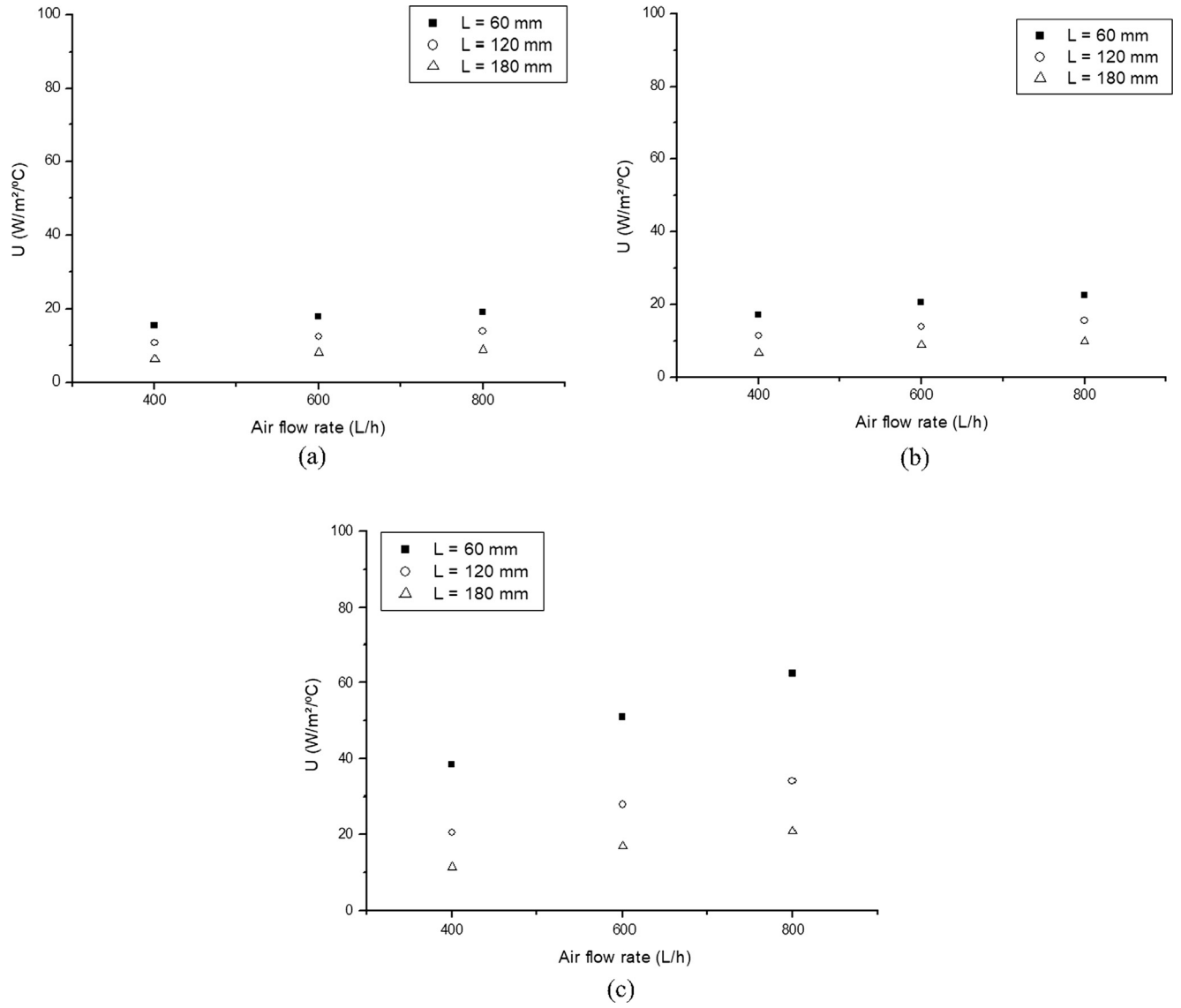

Fig. 10. Global coefficient U at outlet of beds of composed medium referring to T_{avg} integrated over: (a) central region of the bed; (b) full cross-section of the bed; (c) wall-vicinity region of the bed.

Table 2
Global heat transfer coefficient (U) of packed-beds of sugarcane bagasse (SCB) and of composed medium SCB:OPP:WB 1:2:2 w/w (L = 60 mm; α^{*} = 0.05).

Air flow rate (L/h)	U (r/R = 0 to 1)				U (r/R = 0.92 to 1)			
	SCB		SCB:OPP:WB		SCB		SCB:OPP:WB	
	Replicate 1	Replicate 2	Replicate 1	Replicate 2	Replicate 1	Replicate 2	Replicate 1	Replicate 2
400	18.12	15.94	17.66	15.74	37.17	33.88	38.13	37.17
600	22.11	21.07	20.56	18.44	50.51	49.49	49.49	48.52
800	23.70	25.14	21.53	18.58	63.13	68.20	57.86	57.86

Source of variation	GL	F	Valor P	F	Valor P
Porous medium	1	5.96	0.041**	1.67	0.233
Air flow rate	2	11.73	0.004**	71.15	0.000** ($p \ll \alpha = 0.05$)
Error	8				
Total	11				

* α: significance level.
** Source of variation plays significant effect on U (p-value < α).

Based on classical definitions of heat transfer, Eq. (8a) is equivalent to the definition of λ_0. Hence, the assumptions of Sangsurasak and Mitchell (1998) could be contested, once the axial and the radial components of the thermal conductivity tensor are not necessarily equal each other neither equal to the stagnant value, once the dynamic contribution over Λ_r (second term at the right

Table 3
Estimated thermal parameters effective thermal conductivity in radial direction (Λ_r) and wall-to-fluid convective heat transfer coefficient (α_{wall}) for packed-beds of sugarcane bagasse (SCB) and calculated relation Λ_r/λ_0 (λ_0 = stagnant effective thermal conductivity).

Bed height (mm)	Air flow rate (L/h)	Λ_r (W/m/°C)	α_{wall} (W/m^2/°C)	Λ_r/λ_0
60	400	0.09	16.49	1.5
	500	0.21	38.77	3.5
	600	0.25	38.66	4.2
	800	0.25	46.22	4.2
	1000	0.23	53.95	3.9
	1200	0.34	51.76	5.7
120	400	0.11	23.43	1.9
	500	0.12	23.42	2.0
	600	0.13	25.26	2.2
	800	0.13	24.47	2.2
	1000	0.13	29.20	2.2
	1200	0.14	33.73	2.4
180	400	0.06	7.26	1.0
	500	0.07	9.30	1.2
	600	0.08	10.69	1.3
	800	0.07	10.74	1.2
	1000	0.08	12.34	1.3
	1200	0.08	16.09	1.3

Table 4
Estimated thermal parameters Λ_r and α_{wall} for packed-beds of composed medium SCB:OPP:WB 1:2:2 w/w and calculated relation Λ_r/λ_0.

Bed height (mm)	Air flow rate (L/h)	Λ_r (W/m/°C)	α_{wall} (W/m^2/°C)	Λ_r/λ_0
60	400	0.06	35.39	0.9
	600	0.13	49.56	2.0
	800	0.14	52.25	2.1
120	400	0.10	34.28	1.5
	600	0.11	46.34	1.7
	800	0.12	48.87	1.9
180	400	0.06	28.59	1.0
	600	0.08	36.53	1.3
	800	0.09	44.49	1.3

hand-side of Eq. (7a)) would be neglected. However, according to the findings of the current work, we may concern this assumption as a feasible approach for SSF processes in PBBs, since $\Lambda_r \approx \lambda_0$ for the low air flow rates typical of SSF systems.

In PBBs of SSF, many times the air flow rates employed lead to surface velocities even lower than the ones here studied. Umsza-Guez (2009), for instance, has found better results of pectinolytic enzymes production by SSF in a packed-bed with cross-section diameter 76.2 mm using air flow rate 120 L/h. Milagres et al. (2004) found the air flow rate of 48 L/h as optimal for xylanase production using SCB as substrate. Such low surface velocities, although to be necessary to avoid substrate drying, result in a very poor heat exchange due to the dynamic contribution of heat transfer in packed-beds with fluid flow, leading to uncommonly low values of the effective thermal parameters, mainly when the porous matrices are constituted by particles from agricultural waste.

Concerning α_{wall}, the same trend of Λ_r with increasing air flow rate and increasing bed height have been observed. However, values of α_{wall} found in the current work were very low when compared to results from literature (Legawiec and Ziólkowski, 1995; Thoméo, 1990) for similar air flow rates (see Table 5). Such low values reiterate that there is an appreciable convective resistance between the tube wall and the edge of the porous media composed by SCB and by SCB:OPP:WB 1:2:2 w/w. In general, α_{wall} values were higher for PBs of SCB:OPP:WB 1:2:2 w/w than for PBs of SCB, which is attributed to the already discussed structural differences between both porous matrices. Smaller particles of WB and of OPP are supposed to fill the void spaces among SCB fibers, leading to an increase of the turbulence at the near-wall region, as well as breaking the boundary layer. As a result, α_{wall} reached higher values for the beds of composed medium, suggesting a slightly lower (although still appreciable) convective thermal resistance near tube-wall, in comparison with beds of SCB.

Table 5
Values of α_{wall} coefficient from literature.

Particles	G (kg/m^2/s)	α_{wall} (W/m^2/°C)	Reference
Porcelain beads	0.2	65	Tsotsas (2010)
Glass beads	0.4	302	Hamel and Krumm (2008)
	0.9	462	
Sugarcane bagasse	0.2	12	Current work

Moreover, since α_{wall} is strongly dependent on the packing conditions near the wall, as already mentioned, it is therefore to be expected that its value could change appreciably if the bed was packed differently, for instance by a different person. This issue is especially pressing in narrow packed-beds, like the one used in the current paper. Hence, how repeatable are these experiments could be an important question. According to Casciatori et al. (2014), that deeply studied and reported experimental data of several structural properties of beds packed with the same agro-industrial solid by-products applicable to solid-state fermentation also here employed, the reproducibility of the packings is guaranteed. Those authors mention that, even though the accommodation of particles when producing loose packs depends on the operator, the experimental error observed using that packing technique was low (variation coefficient lower than 2%), hence the technique could be considered reproducible.

In Table 6, Λ_r for PBs of SCB and of composed medium with L = 60 mm are presented and statistically compared. Replications refer to parameters estimation based on radial temperature

Table 6
Λ_r of packed-beds of sugarcane bagasse and of composed medium SCB:OPP:WB 1:2:2 w/w (L = 60 mm; α^{*} = 0.05).

Air flow rate (L/h)	Λ_r (W/m/°C)			
	Sugarcane bagasse		Composed medium	
	Replicate 1	Replicate 2	Replicate 1	Replicate 2
400	0.09	0.07	0.06	0.05
600	0.25	0.18	0.13	0.17
800	0.25	0.22	0.14	0.22

Source of variation	Degree of freedom	f-statistic	p-value
Air flow rate	2	22.25	0.001**
Porous medium	1	6.99	0.030**
Error	8		
Total	11		

* α: significance level.
** Source of variation plays significant effect on Λ_r (p-value < α).

profiles obtained in duplicate of independent experiments. Both source of variations, air flow rate and type of porous medium, played significant effect on Λ_r (significance level α = 0.05). Variance analysis confirmed that $\Lambda_{r\ composed\ medium} < \Lambda_{r\ SCB}$. Radial temperature profiles were more defined for composed medium, with higher thermal gradient between r/R = 0.0 and 0.92. Considering Fourier's law for heat conduction, Λ_r of the beds of composed medium had to be smaller than Λ_r of beds of SCB in order to compensate the higher thermal gradients found in the beds of SCB:OPP:WB 1:2:2 w/w. For bed heights L = 120 and 180 mm, same results for this comparison have been found (data not shown).

Finally, in Table 7, confidence intervals (CIs 95% confidence level) are presented for estimated parameters Λ_r and α_{wall} for PBs of SCB and of composed medium with L = 60 mm, in order to show the goodness of the estimation of the parameters by using the traditional two-parameters model (Eq. (4)). According to a parametric sensitivity study developed by Sklivaniotis et al. (1988), Λ_r depends on temperature data obtained in the central region of the bed to be well-estimated, while α_{wall} depends on temperature data obtained in the region near the tube-wall. The flattening of the radial temperature profiles, especially for the PBs of SCB, harmed Λ_r estimation, explaining why CIs are broader for this porous medium, in comparison with SCB:OPP:WB 1:2:2 w/w. Similarly, the convergence of the thermal profiles to a same temperature near tube-wall harmed α_{wall} estimations for PBs of SCB, leading to broad CIs for the estimated values, while for PBs of composed medium the CIs were narrower, but still of same order of magnitude of the parameter estimated. On the above, comparing the two-dimensional with the one-dimensional model, a good choice for studying and modeling heat transfer in packed-beds of agricultural waste applicable to solid-state fermentation might be to employ the one-dimensional model with two regions, determining global coefficients separately for central region of the beds and for wall-vicinity. With this, it is possible to make simulations by using a simple and mathematically easy model that may bring satisfactory results for temperature rises predictions in such bioreactors.

Furthermore, considering the needs of detailed CFD modelling of flows in porous media like the packed-beds of the present work, it is not possible to use the parameter α_{wall} embedded at the thermal boundary condition at r = R. The Navier-Stokes mass and momentum conservation balances, added of additional balances for heat transfer, are solved from the core to the edge of the porous media, while the boundary layer and the wall are out of the domain of the solution. Hence, appropriate boundary conditions must be either Dirichlet (fixed temperature) or Neumann (fixed heat flux) (Dixon and Nijemeisland, 2001). However, α_{wall} may be useful as an output parameter for, jointly with experimental thermal profiles, validate CFD simulations.

Anyhow, the interpretations of α_{wall} in the context of CFD or in the current paper are not the same. In the present approach, α_{wall} is a lumped parameter that addresses the extra resistance near the wall when the bed is viewed as a single-phase continuum (pseudo-homogeneous model); in practice, temperature differences between the fluid and the solid phases are neglected. The use of the convective boundary condition helps to explain the measured 'temperature jump' near the wall (Logtenberg et al., 1999). In CFD, it is possible to resolve heat transfer in parallel for fluid and solid phases. As a general practice, the heat transfer coefficients are used as discussed in the review paper of Deen et al. (2014). In summary, it is possible to increase complexity further in CFD simulations, but then the particulate phase must be resolved in detail, specifying contact area and contact heating at these positions. Once the particles composing porous media applied to SSF are usually highly non-regular in shape and size, making difficult the definition of an appropriate mesh for CFD application, the classical approaches here studied, either the traditional two-parameters or even the one-dimensional model, may still work quite well.

4. Conclusions

The analysis of radial temperature profiles at outlet of beds packed with particles of agricultural waste typically used as substrates in solid-state fermentation packed-bed bioreactors makes to presume that dissipating reactional or metabolically generated heat from within those bioreactors is a challenge due to the combination of two main factors that disfavor heat transfer: low effective thermal conductivity and low wall-to-fluid convective coefficient of heat transfer. The low air flow rates, that have to be employed in order to avoid drying of the porous media, make both thermal conductive and convective coefficients to be near stagnant heat transfer parameters. Additionally, the agro-industrial waste are naturally non-conductive materials. The parameters estimated in the current paper can be used for more realistic predictions of thermal fields in solid-state fermentation processes conducted in bioreactors packed with the studied materials and percolated by low air flow rates.

Table 7
Confidence intervals (CI 95%) of the parameters estimated (L = 60 mm).

Air flow rate (L/h)	Sugarcane bagasse		Composed medium	
	Λ_r (W/m/°C) (CI 95%)	α_{wall} (W/m^2/°C) (CI 95%)	Λ_r (W/m/°C) (CI 95%)	α_{wall} (W/m^2/°C) (CI 95%)
400	0.09 (±0.04)	16.49 (±9.94)	0.06 (±0.01)	35.39 (±20.26)
600	0.25 (±0.12)	38.66 (±24.54)	0.13 (±0.01)	49.57 (±25.16)
800	0.25 (±0.14)	46.22 (±37.28)	0.14 (±0.03)	52.25 (±7.33)

Acknowledgments

The authors gratefully acknowledge the funding of this work by the Coordination for the Improvement of Higher Education Personnel (CAPES) and by São Paulo Research Foundation (FAPESP) (Grants #2008/55736-3; #2011/07453-5; #2012/13939-0; #2014/25183-3, #2014/23453-3 and #2018/00996-2).

References

Ashley, V.M., Mitchell, D.A., Howes, T., 1999. Evaluating strategies for overcoming overheating problems during solid-state fermentation in packed beds bioreactors. Biochem. Eng. J. 3, 141–150.

Augier, F., Idoux, F., Delenne, J.Y., 2010. Numerical simulations of transfer and transport properties inside packed beds of spherical particles. Chem. Eng. Sci. 65, 1055–1064.

Bird, R.B., Stewart, W.E., Lightfoot, E.N., 2002. Fenômenos de Transporte. LTC, Rio de Janeiro.

Casciatori, F.P., Laurentino, C.L., Lopes, K.C.M., Souza, A.G., Thoméo, J.C., 2013. Stagnant effective thermal conductivity of agro-industrial residues for solid state fermentation. Int. J. Food Prop. 16, 1578–1593.

Casciatori, F.P., Laurentino, C.L., Taboga, S.R., Casciatori, P.A., Thoméo, J.C., 2014. Structural properties of beds packed with agro-industrial solid by-products applicable for solid-state fermentation: experimental data and effects on process performance. Chem. Eng. J. 255, 214–224.

Casciatori, F.P., Bück, A., Thoméo, J.C., Tsotsas, E., 2016. Two-phase and two-dimensional model describing heat and water transfer during solid-state fermentation within a packed-bed bioreactor. Chem. Eng. J. 287, 103–116.

Coberly, C.A., Marshall, W.R., 1951. Temperature gradients in gas streams flowing through fixed granular beds. Chem. Eng. Progress 47, 141–150.

Colburn, A.P., 1931. Heat transfer in packed tubes. Ind. Eng. Chem. 32, 910–913.

de Wash, A.P., Froment, G.F., 1972. Heat-transfer in packed-beds. Chem. Eng. Sci. 27, 567–576.

Deen, N.G., Peters, E.A.J.F., Padding, J.T., Kuipers, J.A.M., 2014. Review of direct numerical simulation of fluid-particle mass, momentum and heat transfer in dense gas-solid flows. Chem. Eng. Sci. 116, 710–724.

Dixon, A.G., 1985. The length effect on packed bed effective heat transfer parameters. Chem. Eng. J. 31, 163–173.

Dixon, A.G., 1997. Heat transfer in fixed beds at very low (<4) tube-to-particle diameter ratio. Ind. Eng. Chem. Res. 36, 3053–3064.

Dixon, A.G., Nijemeisland, M., 2001. CFD as a design tool for fixed-bed reactors. Ind. Eng. Chem. Res. 40, 5246–5254.

Dixon, A.G., Paterson, W.R., Creswell, D.L., 1978. Heat transfer in packed beds of low tube/particle diameter ratio. ACS Symp. Ser. 65, 238–253.

Durand, A., de la Broise, D., Blachere, H., 1998. Laboratory scale bioreactor for solid-state process. J. Biotechnol. 59–66.

Fanaei, M.A., Vaziri, B.M., 2009. Modeling of temperature gradients in packed-bed solid-state bioreactors. Chem. Eng. Process. 48, 446–451.

Freiwald, M.G., Paterson, W.R., 1992. Accuracy of model predictions and reliability of experimental data for heat transfer in packed beds. Chem. Eng. Sci. 47, 1545–1560.

Ghildyal, N.P., Gowthaman, M.K., Raghavarao, K.S.M.S., Karanth, N.G., 1994. Interaction of transport resistances with biochemical reaction in packed-bed solid-state fermentors: effect of temperature gradients. Enz. Microb. Technol. 16, 253–257.

Guardo, A., Coussirat, M., Larrayoz, M.A., Recasens, F., Egusquiza, E., 2005. Influence of the turbulence model in CFD modeling of wall to fluid heat transfer in packed beds. Chem. Eng. Sci. 60, 1733–1742.

Gunn, D.J., Ahmad, M.M., Sabri, M.N., 1987. Radial heat transfer to fixed beds of particles. Chem. Eng. Sci. 42, 2163–2171.

Hamel, S., Krumm, W., 2008. Near-wall porosity characteristics of fixed beds packed with wood chips. Powder Technol. 188, 55–63.

Kunii, D., Suzuki, M., 1967. Particle to fluid heat and mass transfer in packed beds of fine particles. Int. J. Heat Mass Transfer 10, 845–852.

Laurentino, C.L., 2007. Transferência de calor em leitos fixos com aplicação em reatores de fermentação em estado sólido, MSc. Dissertation, PPG-ECA/UNESP, São José do Rio Preto; 2007.

Legawiec, B., Ziólkowski, D., 1995. Mathematical simulation of heat transfer within tubular flow apparatus with packed bed by a model considering system inhomogeneity. Chem. Eng. Sci. 50, 673–683.

Logtenberg, S.A., Nijemeisland, M., Dixon, A.G., 1999. Computational fluid dynamics simulations of fluid flow and heat transfer at the wall-particle contact points in a fixed-bed reactor. Chem. Eng. Sci. 54, 2433–2439.

Marquardt, D.W., 1963. An algorithm for least squares estimation of nonlinear parameters. SIAM J. Appl. Math. 11, 431–441.

Martin, N., de Souza, S.R., da Silva, R., Gomes, E., 2004. Pectinase production by fungal strains in solid-state fermentation using agro-industrial bioproduct. Braz. Arch. Biol. Technol. 47, 813–819.

Martin, N., Guez, M.A.U., Sette, L.D., da Silva, R., Gomes, E., 2010. Pectinase production by a Brazilian thermophilic fungus *Thermomucor indicae-seudaticae* N31 in solid-state and submerged fermentation. Microbiology 79, 306–313.

Milagres, A.M.F., Santos, E., Piovan, T., Roberto, I.C., 2004. Production of xylanase by *Thermoascus aurantiacus* from sugar cane bagasse in an aerated growth fermentor. Process Biochem. 39, 1387–1391.

Mitchell, D.A., Pandey, A., Sangsurasak, P., Krieger, N., 1999. Scale-up strategies for packed bed bioreactors for solid state fermentation. Proc. Biochem. 35, 167–178.

Mitchell, D.A., Krieger, N., Stuart, D.M., Pandey, A., 2000. New developments in solid-state fermentation. II. Rational approaches to the design, operation and scale up of bioreactors. Process Biochem. 35, 1211–1225.

Pandey, A., 1992. Recent process-developments in solid-state fermentation. Proc. Biochem. 27, 109–117.

Ridgway, K., Tarbuck, K.J., 1968. Voidage fluctuations in randomly-packed bed of spheres adjacent to a containing wall. Chem. Eng. Sci. 23, 1147–1155.

Sangsurasak, P., Mitchell, D.A., 1995b. The investigation of transient multidimensional heat transfer in solid state fermentation. Chem. Eng. J. 60, 199–204.

Sangsurasak, P., Mitchell, D.A., 1995a. Incorporation of death kinetics into a 2-D dynamic heat transfer model for solid state fermentation. J. Chem. Technol. Biotechnol. 64, 253–260.

Sangsurasak, P., Mitchell, D.A., 1998. Validation of a model describing two-dimensional heat transfer during solid-state fermentation in packed bed bioreactors. Biotechnol. Bioeng. 60, 739–749.

Saucedo-Castañeda, G., Gutiérrez-Rojas, M., Bacquet, G., Raimbault, M., Viniegra-González, G., 1990. Heat transfer simulation in solid substrate fermentation. Biotechnol. Bioeng. 35, 802–808.

Sklivaniotis, M., Castro, J.A.A., Mc Greavy, C., 1988. Characteristic features of parametric sensitivity in a fixed bed heat exchanger. Chem. Eng. Sci. 43, 1517–1522.

Smirnov, E.I., Muzykantov, A.V., Kuzmin, V.A., Kronberg, A.E., Zolotarskii, I.A., 2003. Radial heat transfer in packed beds of spheres, cylinders and Rashig rings: verification of model with a linear variation of λ_{er} in the vicinity of the wall. Chem. Eng. J. 91, 243–248.

Soccol, C.R., 1995. Aplicações da fermentação no estado sólido na valorização de produtos e resíduos agroindustriais. Integração pesquisa-indústria no setor agroalimentar. http://www.cendotec1.org.br/ffantigos/ff04a.pdf, (accessed 3rd Aug 2006).

Thoméo, J.C., Freire, J.T., 2000. Heat transfer in fixed bed: a model non-linearity approach. Chem. Eng. Sci. 55, 2329–2338.

Thoméo, J.C., Freire, J.T., 2012. Experimental and modeling aspects of heat transfer in packed beds. In: Freire, J.T., Silveira, A.M., Ferreira, M.C. (Eds.), Transport Phenomena on Particulate Systems, (ebook). Bentham Sci. Pub, Oak Park.

Thoméo, J.C., Grace, J.R., 2004. Heat transfer in packed beds: experimental evaluation of one-phase water flow. Braz. J. Chem. Eng. 21, 13–22.

Thoméo, J.C., Rouiller, C.O., Freire, J.T., 2004. Experimental analysis of heat transfer in packed beds with air flow. Ind. Eng. Chem. Res. 43, 4140–4148.

Thoméo, J.C., 1990. Análise experimental dos efeitos de entrada térmicos sobre os coeficientes de transferência de calor em leito fixo, MSc. Dissertation, PPG-EQ/UFSCar, São Carlos.

Thoméo, J.C., 1995. Transferência de calor em leito fixo: o modelo a dois parâmetros tradicional revisitado, PhD. Thesis, PPG-EQ/UFSCar, São Carlos.

Tsotsas, E., 2010. Thermal conductivity of packed beds. In: VDI Heat Atlas, Springer Verlag: Berlin.

Umsza-Guez, M.A., 2009. Produção de poligalacturonase em fermentação em estado sólido pelo fungo Thermomucor indicae-seudaticae N31 em escala de frascos e biorreator de leito fixo, PhD. Thesis, PPG-ECA/UNESP, São José do Rio Preto.

Von Meien, O.F., Mitchell, D.A., 2002. A two-phase model for water and heat transfer within an intermittently-mixed solid-state fermentation bioreactor with forced aeration. Biotechnol. Bioeng. 79, 416–428.

Wen, D., Ding, Y., 2006. Heat transfer of gas flow through a packed bed. Chem. Eng. Sci., 3532–3542

Zotin, F.M.Z., 1985. O efeito parede em colunas de recheio, MSc. Dissertation, PPG-EQ/UFSCar, São Carlos.